INEEL/EXT-05-02658

Implementation of Molten Salt Properties into RELAP5-3D/ATHENA

January 2005

Idaho National Engineering and Environmental Laboratory
Bechtel BWXT Idaho, LLC

INEEL/EXT-05-02658

Implementation of Molten Salt Properties into RELAP5-3D/ATHENA

Cliff B. Davis

January 2005

Idaho National Engineering and Environmental Laboratory
Idaho Falls, Idaho 83415

EXECUTIVE SUMMARY

Molten salts are being considered as coolants for the Next Generation Nuclear Plant (NGNP) in both the reactor and the heat transport loop between the reactor and the hydrogen production plant because of their superior thermophysical properties compared to helium. Because specific molten salts have not been selected for either application, four separate molten salts were implemented into the RELAP5-3D/ATHENA computer program as working fluids. The implemented salts were LiF-BeF_2 in a molar mixture that is 66% LiF and 34% BeF_2, respectively, $NaBF_4$-NaF (92% and 8%), LiF-NaF-KF (11.5%, 46.5%, and 42%), and NaF-ZrF_4 (50% and 50%). LiF-BeF_2 is currently the first choice for the primary coolant for the Advanced High-Temperature Reactor, while NaF-ZrF_4 is being considered as an alternate. $NaBF_4$-NaF and LiF-NaF-KF are being considered as possible coolants for the heat transport loop.

The molten salts were implemented into ATHENA using a simplified equation of state based on data and correlations obtained from Oak Ridge National Laboratory. The simplified equation of state assumes that the liquid density is a function of temperature and pressure and that the liquid heat capacity is constant. The vapor is assumed to have the same composition as the liquid and is assumed to be a perfect gas.

The implementation of the thermodynamic properties into ATHENA for LiF-BeF_2 was verified by comparisons with results from a detailed equation of state that utilized a soft-sphere model. The comparisons between the simplified and soft-sphere models were in reasonable agreement for liquid. The agreement for vapor properties was not nearly as good as that obtained for liquid. Large uncertainties are possible in the vapor properties because of a lack of experimental data. The simplified model used here is not expected to be accurate for boiling or single-phase vapor conditions. Because neither condition is expected during NGNP applications, the simplified equation of state is considered acceptably accurate for analysis of the NGNP.

CONTENTS

TABLES

FIGURES

NOMENCLATURE

Symbol	Parameter
A	Constant that depends on the salt composition
B	Constant that depends on the salt composition
c_P	Specific heat capacity at constant pressure (J/kg-K)
$\tilde{c}_P$	Molar specific heat capacity at constant pressure (J/mole-K)
k	Thermal conductivity (W/m-K)
M	Molecular weight (g/mole)
T	Temperature (K)
P	Pressure (Pa)
Q	Heat per unit mass (J/kg)
R	Gas constant (J/kg-K)
$\overline{R}$	Universal gas constant (8.31434 J/mole-K)
s	Specific entropy (J/kg-K)
u	Specific internal energy (J/kg)
v	Specific volume (m^3/kg)
$\tilde{V}$	Volume of the solid phase at melting (cm^3/mole)
W	Work per unit mass (J/kg)
X_i	Mole fraction
x_i	Mass fraction
β	Coefficient of thermal expansion (1/K)
κ	Isothermal compressibility (1/Pa)
ε/K	Potential constant (K)
μ	Dynamic viscosity (Pa-s)
ρ	Density (kg/m^3)
σ	Surface tension (N/m)
σ_i	Collision diameter, $\overset{o}{A}$
Φ_{ij}	Weighting factor

1. INTRODUCTION

The RELAP5-3D© program (INEEL 2003) is being developed to simulate thermal-hydraulic transients in reactor systems that use light water as the working fluid. The ATHENA code is incorporated as a compile-time option in RELAP5-3D that generalizes the capability of the code to simulate systems that use working fluids other than water. Molten salts are being considered as coolants for the Next Generation Nuclear Plant (NGNP) in both the reactor and the heat transport loop between the reactor and the hydrogen production plant because of their superior thermophysical properties compared to helium. Because specific molten salts have not been selected for either application, four separate molten salts were incorporated into ATHENA as working fluids. The salts incorporated into ATHENA were LiF-BeF_2 in a molar mixture that is 66% LiF and 34% BeF_2, respectively, $NaBF_4$-NaF (92% and 8%), LiF-NaF-KF (11.5%, 46.5%, and 42%), and NaF-ZrF_4 (50% and 50%). The salts LiF-BeF_2 and LiF-NaF-KF are also known as Flibe and Flinak, respectively. LiF-BeF_2 is currently the first choice for the primary coolant for the Advanced High-Temperature Reactor, while NaF-ZrF_4 is being considered as an alternate (Ingersoll et al. 2004). $NaBF_4$-NaF and LiF-NaF-KF are being considered as possible coolants for the heat transport loop. The primary range of interest for NGNP applications is from 773 to 1273 K.

The implementation of a new fluid into ATHENA is generally performed using a detailed equation of state to generate fluid properties. Chen et al. (1992a) developed an equation of state for LiF-BeF_2 based on a soft-sphere model. The soft-sphere model was used to generate LiF-BeF_2 properties for use in the fusion safety program (Moore 2000). The fusion property generator was easily converted for use with ATHENA. However, preliminary applications of the fusion generator resulted in non-convergence when the pressure exceeded 2.4 MPa. The non-convergence was not a problem for fusion applications, where the primary interest was at low pressure, but was of concern for NGNP applications, where higher pressures could be obtained during transients. Consequently, the molten salts were implemented into ATHENA using a simplified equation of state based on data obtained from Oak Ridge National Laboratory (ORNL). The simplified equation of state, which was similar to one used by Sabharwall et al. (2004) in an older version of ATHENA, was easily extended to higher pressures and temperatures. Furthermore, the simplified equation of state was easily converted to represent the other molten salts ($NaBF_4$-NaF, LiF-NaF-KF, and NaF-ZrF_4) for which no detailed equation of state was available.

The use of a simplified equation of state for implementing the molten salts into ATHENA was complicated by a lack of experimental data. For example, vapor pressure curves were available for only two of the four salts and property data for the vapor phases were non-existent. Although vapor property data are not important for NGNP applications, with the relatively minor exception of a small amount of salt vapor in a noncondensable cover gas, vapor property data are required by ATHENA because of its origins for simulating two-phase phenomena in light water.

The simplified equation of state assumes that the liquid density is a function of temperature and pressure based on correlations developed by ORNL and that the liquid heat capacity is constant. The vapor is assumed to have the same composition as the liquid and is assumed to be a perfect gas. One limitation of the simplified equation of state is that it cannot accurately represent the entire thermodynamic range of possible pressures and temperatures, which results in discontinuities near the critical point. This limitation should not be too serious for NGNP applications, where boiling will be avoided and the state should remain far from critical.

The remainder of this report describes the fluid properties for the four molten salts, the verification of the implemented fluid properties, the code modifications that were made to ATHENA, the quality assurance, conclusions, and references.

2. FLUID PROPERTIES

ATHENA accesses salt thermodynamic properties through tables located in auxiliary files called 'tpfms1' for the first molten salt, 'tpfms2' for the second molten salt, and so forth. The required fluid properties include specific volume, v (m^3/kg); specific internal energy, u (J/kg); coefficient of thermal expansion, β (1/K); isothermal compressibility, κ (1/Pa); specific heat capacity at constant pressure, c_P (J/kg-K); and specific entropy, s (J/kg-K). The coefficient of thermal expansion and isothermal compressibility are defined as

$$\beta \equiv \frac{1}{v}\left(\frac{dv}{dT}\right)_P = -\frac{1}{\rho}\left(\frac{d\rho}{dT}\right)_P \tag{1}$$

and

$$\kappa \equiv -\frac{1}{v}\left(\frac{dv}{dP}\right)_T = \frac{1}{\rho}\left(\frac{d\rho}{dP}\right)_T, \tag{2}$$

where T is the temperature (K), P is the pressure (Pa), and ρ is the density (kg/m^3).

The calculation of these properties for the liquid and vapor phases are described in Sections 2.1 and 2.2, respectively. The properties required to define the saturation line are described in Section 2.3. Transport properties are described in Section 2.4.

2.1 Liquid Thermodynamic Properties

Powers et al. (1963), Cantor et al. (1968), and Cantor (1973) present correlations for the liquid density of the form

$$\rho_T = A_D(T - 273.15) + B_D\ , \tag{3}$$

where ρ_T is the density as a function of temperature and A_D and B_D are constants that depend on the salt. Cantor et al. (1968) also present correlations for the isothermal compressibility of LiF-BeF_2 and $NaBF_4$-NaF that have the form

$$\kappa = A_\kappa e^{B_\kappa T}, \tag{4}$$

where A_κ and B_κ are constants. The simplified equation of state used here represents the effects of temperature and pressure on liquid density as

$$\rho = \rho_T[1 + \kappa(P - P_0)], \tag{5}$$

where P_0 is a reference pressure that is defined in Section 2.3. Although the isothermal compressibility is small for a liquid, and could be neglected, the use of Equation (5) allows a

more consistent calculation of the density and the isothermal compressibility than would be obtained using only Equation (3). The isothermal compressibility is calculated from Equation (4) rather than by combining Equations (2) and (5). The difference is small (<1%) and using Equation (4) allows the isothermal compressibility to remain a function of temperature alone, consistent with the ORNL correlation.

The specific volume, which is required by ATHENA, is calculated as

$$v = \frac{1}{\rho} \quad . \tag{6}$$

Table 1 summarizes the liquid properties for the four salts implemented into ATHENA, including their composition and melting temperature, T_{melt}. The density constants used in Equation (3) are also listed in the table. These density constants were based on experimental data taken between 788 and 1093 K for LiF-BeF_2 and between 673 and 864 K for $NaBF_4$-NaF. The experimental range for the other salts is not known. Estimates of uncertainty vary between 2% (Cantor et al. 1968) and 5% (Powers et al. 1963).

Table 1. Constants for liquid salts.

Salt	Composition (mole fraction)	T_{melt} (K)	A_D (kg/m^3-K)	B_D (kg/m^3)	A_κ (1/Pa)	B_κ (1/K)	c_P (J/kg-K)
1	LiF-BeF_2 (0.66, 0.34) [a]	731.15[a]	-0.4884[b]	2279.7[b]	2.3E-11 [a]	0.001[a]	2386[a]
2	$NaBF_4$-NaF (0.92, 0.08) [a]	658.15[a]	-0.7110[b]	2252.1[b]	9.0E-11 [a]	0.0016[a]	1507[a]
3	LiF-NaF-KF (0.115, 0.465, 0.42) [c]	727.15[c]	-0.73[c]	2530[c]	NA[d]	NA[d]	1884[c]
4	NaF-ZrF_4 (0.50, 0.50) [c]	783.15[c]	-0.93[c]	3790[c]	NA[d]	NA[d]	1151[c]

a. From Cantor et al. (1968).
b. From Cantor (1973).
c. From Powers et al. (1963).
d. Not available. The constants were set to the values for LiF-BeF_2.

The constants used to calculate the isothermal compressibility from Equation (4) are also listed in Table 1. The correlations for LiF-BeF_2 and $NaBF_4$-NaF were based on estimates by Cantor et al. (1968). They estimated that the uncertainty was a factor of 3 and indicated that the correlations were less reliable for pressures exceeding 5 MPa. Correlations were not available for the other molten salts. The constants for these salts were arbitrarily set to the values for LiF-BeF_2.

The coefficient of thermal expansion was calculated using Equations (1), (3), (4), and (5) to obtain

$$\beta = -\left(\frac{A_D}{\rho_T} + \frac{B_\kappa \kappa (P - P_0)}{1 + \kappa (P - P_0)} \right) \quad . \tag{7}$$

The specific heat capacity for each molten salt is also given in Table 1. Cantor et al. (1968) estimated an uncertainty of 3% for LiF-BeF_2 and 2% for $NaBF_4$-NaF. Powers et al. (1963) estimated an uncertainty of 10% for the other molten salts.

The change in specific internal energy from a reference state to a given pressure, P, and temperature, T, was calculated as the sum of two steps. The process consisted of a reversible, isothermal change in pressure from the reference pressure, P_0, to the given pressure followed by a reversible, isobaric change in temperature from the reference temperature, T_0, to the given temperature. For the first step, the change in specific internal energy, Δu_1, is (Zemansky 1968)

$$\Delta u_1 = Q - W = -T\int_{P_0}^{P} v\beta dP - \int_{P_0}^{P} - v\kappa P dP , \tag{8}$$

where Q is the heat added to the fluid per unit mass and W is the work performed by the fluid per unit mass during the process. Because the values inside the integrals are nearly independent of pressure for a liquid, they are treated as constants yielding

$$\Delta u_1 \approx -T\bar{v}\bar{\beta}(P - P_0) + 0.5\bar{v}\bar{\kappa}(P^2 - {P_0}^2) , \tag{9}$$

where the overscore denotes that average values are used. Note that an exact integration of Equation (8) could have been performed because the functional forms of the parameters inside the integral were explicitly specified. However, the differences between Equation (9) and the exact solution are not significant.

The specific internal energy change for the second step in the process, Δu_2, was calculated applying the first law of thermodynamics and assuming that the specific heat capacity was constant. During the isobaric process (Zemansky 1968),

$$\Delta u_2 = c_P(T - T_0) - P(v - v_1) , \tag{10}$$

where v and v_1 are evaluated from Equation (6) at P and T and P and T_0, respectively. The specific internal energy is then calculated as

$$u = u_{f0} + \Delta u_1 + \Delta u_2 , \tag{11}$$

where u_{f0} is a reference liquid specific internal energy that is evaluated at P_0 and T_0.

The specific entropy is calculated similarly as (Zemansky 1968)

$$\Delta s_1 = -\int_{P_0}^{P} \beta v dP \approx -\bar{\beta}\bar{v}(P - P_0) \tag{12}$$

$$\Delta s_2 = \int_{T_0}^{T} \frac{c_P}{T} dT = c_P \ln(T/T_o) \tag{13}$$

and

$$s = s_{f0} + \Delta s_1 + \Delta s_2 , \tag{14}$$

where s_{f0} is a reference liquid specific entropy that is evaluated at P_0 and T_0.

2.2 Vapor Thermodynamic Properties

References presenting measurements or correlations for physical properties of salt vapors were not located. Consequently, vapor thermodynamic properties were calculated using perfect gas relationships, which imply that the specific internal energy is a function of temperature alone and that the specific heat capacity is constant. The composition of the vapor is also assumed to be the same as that of the liquid. As mentioned previously, vapor properties are not expected to be important for NGNP applications so approximate methods are considered satisfactory. Large uncertainties should be expected if ATHENA is applied to conditions where the vapor properties are important.

The molecular weight, M, of the gas mixture is calculated as (Zucrow and Hoffman 1976)

$$M = \sum_i X_i M_i \quad , \tag{15}$$

where M_i is the molecular weight of the i^{th} component in the mixture and X_i is the corresponding mole fraction given in Table 1. The gas constant for the mixture, R, is calculated as

$$R = \frac{\overline{R}}{M} \quad , \tag{16}$$

where $\overline{R}$ is the universal gas constant. The specific volume of the vapor is calculated using an ideal gas relationship

$$v = \frac{RT}{P} \quad . \tag{17}$$

The coefficient of thermal expansion is calculated by combining Equations (1) and (17) to obtain

$$\beta = \frac{1}{T} \quad . \tag{18}$$

Similarly, the isothermal compressibility is calculated as

$$\kappa = \frac{1}{P} \quad . \tag{19}$$

The mass fraction, x_i, of each component in the mixture is calculated as

$$x_i = \frac{X_i M_i}{M} \tag{20}$$

and is used to calculate the specific heat capacity of the mixture

$$c_P = \sum_i x_i c_{P_i} \qquad (21)$$

(Zucrow and Hoffman 1976).

The parameters used for the individual components contained in the molten salts are given in Table 2. These parameters include the molecular weight, M_i, and the molar specific heat capacity, $\tilde{c}_{P_i}$. The specific heat capacity is treated as a constant even though Chase (1998) and Knacke et al. (1991) show that it varies somewhat with temperature. The specific heat capacity varies by less than +/- 5% between 800 and 1300 K, which encompasses the range of interest for the NGNP.

Table 2. Parameters for vapor components.

Component	M_i (g/mole)	$\tilde{c}_{P_i}$ (J/mole-K)
LiF	25.939[a]	36.888[b]
BeF_2	47.009[a]	58.728[b]
$NaBF_4$	109.808[c]	112.989[c]
NaF	41.988[a]	37.699[b]
KF	58.097[a]	37.846[b]
ZrF_4	167.214[a]	105.459[b]

a. From Chase (1998).
b. From Chase (1998). The specific heat capacity was evaluated at 1000 K.
c. The specific heat capacity of $NaBF_4$ was calculated assuming an equimolar mixture of NaF and BF_3 (Knacke et al. 1991) using Equations (15), (20), and (21). The specific heat capacity of BF_3 was obtained from Knacke et al. (1991) at 1000 K and was 75.29 J/mole-K. The molecular weight of BF_3 was obtained from Glasstone and Sesonske (1967) and was 67.820 g/mole.

The constants for the vapor mixtures are summarized in Table 3. The table includes the molecular weight calculated from Equation (15), the gas constant calculated from Equation (16), and the specific heat capacity calculated from Equation (21).

Table 3. Constants for salt vapors.

Salt	Composition (mole fraction)	M (g/mole)	R (J/kg-K)	c_P (J/kg-K)
1	$LiF\text{-}BeF_2$ (0.66, 0.34)	33.103	251.17	1339.
2	$NaBF_4$-NaF (0.92, 0.08)	104.383	79.653	1025.
3	LiF-NaF-KF (0.115, 0.465, 0.42)	46.908	177.25	803.0
4	$NaF\text{-}ZrF_4$ (0.50, 0.50)	104.601	79.486	684.3

The change in specific internal energy from a reference state to a given pressure, P, and temperature, T, is calculated as the sum of two steps. The process consists of an isobaric change in temperature from the reference temperature, T_0, to the given temperature followed by a isothermal change in pressure from the reference pressure, P_0, to the given pressure. For the first step, the change in specific internal energy, Δu_1, is (Zucrow and Hoffman 1976)

$$\Delta u_1 = \int_{T_0}^{T} (c_p - R)dT = (c_P - R)(T - T_0). \tag{22}$$

The specific internal energy change for the second step in the process, Δu_2, is

$$\Delta u_2 = 0 \tag{23}$$

because the specific internal energy does not depend on pressure for a perfect gas. The specific internal energy is then calculated as

$$u = u_{g0} + \Delta u_1 + \Delta u_2 \ , \tag{24}$$

where u_{g0} is a reference vapor specific internal energy that is evaluated at P_0 and T_0.

The specific entropy is calculated as (Zucrow and Hoffman 1976)

$$\Delta s_1 = \int_{T_0}^{T} \frac{c_P dT}{T} = c_P \ln(T/T_0) \tag{25}$$

$$\Delta s_2 = -\int_{P_0}^{P} \frac{R}{P} dP = - R\ln(P/P_0) \tag{26}$$

and

$$s = s_{g0} + \Delta s_1 + \Delta s_2 \tag{27}$$

where s_{g0} is a reference gas specific entropy that is evaluated at P_0 and T_0.

2.3 Saturation Line

Cantor et al. (1968) present correlations for the vapor pressure that have the form

$$P_{sat} = 133.32 \times 10^{(A_{sat} - B_{sat}/T)} \tag{28}$$

where the subscript sat refers to saturation conditions and A_{sat} and B_{sat} are constants that depend on the salt. The uncertainty in the vapor pressure was estimated to be a factor of 10 from 773 to 973 K for LiF-BeF_2 and 10% from 673 to 973 K for $NaBF_4$-NaF.

Solving Equation (29) for the saturation temperature, T_{sat}, yields

$$T_{sat} = \frac{B_{sat}}{A_{sat} + \log_{10}(133.32) - \log_{10}(P)} \quad . \tag{29}$$

Cantor et al. (1968) presents values for the constants A_{sat} and B_{sat} for LiF-BeF_2 and $NaBF_4$-NaF as shown in Table 4. Values are not available for the other salts.

Table 4. Saturation line constants.

Salt	Composition	A_{sat}	B_{sat} (K)
1	LiF-BeF_2	9.04	10500
2	$NaBF_4$-NaF	9.024	5920
3	LiF-NaF-KF	NA[a]	NA[a]
4	NaF-ZrF_4	NA[a]	NA[a]

a. Not available. The constants were set to the values for LiF-BeF_2.

The saturation line was used to define the triple and critical points. The triple point temperature was set to the melting temperature given in Table 1. The triple point pressure was then calculated from the triple point temperature using Equation (28). The reference values of T_0 and P_0 used previously were set to the triple point values.

The critical point was also defined using the saturation line. First, the temperature of the boiling point, T_{boil}, was calculated from Equation (29) at atmospheric pressure. The critical temperature, T_{crit}, was then estimated from empirical relations given by Bird et al. (1960)

$$T_{crit} = \frac{1.15}{0.77} T_{boil} = 1.494 T_{boil} \quad . \tag{30}$$

The critical pressure was then calculated from the critical temperature using Equation (28).

The resulting values for the triple and critical points are given in Table 5. The uncertainties in the estimated critical conditions are large because Equation (30) is empirical, large extrapolations in the vapor pressure curves are required for LiF-BeF_2 and $NaBF_4$-NaF, and vapor pressure curves are not available for the other salts. For example, Chen et al. (1992a) predicted critical values of 4498.8 K and 19.85 MPa for LiF-BeF_2 using the soft sphere model, which are more than two times and ten times the corresponding values presented in Table 5. The critical values from the soft-sphere model were not used here because they were inconsistent with the available vapor curve after the required extrapolation. Furthermore, no critical values were available for the other molten salts. The uncertainty in the critical conditions should not be too much of a concern for

NGNP applications, where expected temperatures are much below the critical values shown in Table 5.

Table 5. Values for the triple and critical points.

Salt	Composition	T_0 (K)	P_0 (Pa)	T_{crit} (K)	P_{crit} (Pa)
1	$LiF\text{-}BeF_2$	731.15	6.367E-4	2138.9	1.8023E6
2	$NaBF_4\text{-}NaF$	658.15	142.6	1439.8	10.895E6
3	LiF-NaF-KF	727.15	5.308E-4	2138.9	1.8023E6
4	$NaF\text{-}ZrF_4$	783.15	5.721E-3	2138.9	1.8023E6

Table 6 gives reference values for the specific internal energy and specific entropy referred to in Equations (11), (14), (24), and (27). The reference values correspond to the liquid and vapor states at the triple point. The liquid values were set to zero at the triple point. The vapor values were set so that the difference between the vapor and liquid values were approximately zero at the critical point. Other fluid properties will exhibit large discontinuities when going from the liquid phase to the vapor phase near the critical point. Thus, calculations near the critical point should be avoided.

Table 6. Reference values for specific internal energy and specific entropy.

Salt	Composition	u_{f0} (J/kg)	s_{f0} (J/kg-K)	u_{g0} (J/kg)	s_{g0} (J/kg-K)
1	$LiF\text{-}BeF_2$	0.0	0.0	1.827E6	6590
2	$NaBF_4\text{-}NaF$	0.0	0.0	4.358E5	1271
3	LiF-NaF-KF	0.0	0.0	1.775E6	5056
4	$NaF\text{-}ZrF_4$	0.0	0.0	7.402E5	2024

2.4 Transport Properties

ATHENA requires five transport properties for each fluid, including liquid dynamic viscosity, liquid thermal conductivity, surface tension, vapor dynamic viscosity, and vapor thermal conductivity.

Cantor et al. (1968), Cantor (1973), and Powers et al. (1963) present correlations for the liquid dynamic viscosity, μ, that have the form

$$\mu = A_\mu e^{(B_\mu/T)} \tag{31}$$

where A_μ and B_μ are constants that vary between salts. The uncertainty is estimated to be between 10% (Powers et al. 1963) and 15% (Cantor et al. 1968). The correlation for $NaBF_4$-NaF was based on data taken between 682 and 810 K (Cantor 1973). The correlation for LiF-NaF-KF

applies between 773 and 1073 K (Powers 1963). The correlation for NaF-ZrF_4 applies between 873 and 1073 K (Powers 1963). A range was not given for LiF-BeF_2, but it is expected to be similar to the other salts.

ORNL reports constant values for the liquid thermal conductivity, k. Estimates of uncertainty vary from 10% to 50% (Cantor et al. 1968). The constants for the transport properties of the liquid salts are given in Table 7.

Table 7. Constants for transport properties of liquid.

Salt	Composition	A_μ (Pa-s)	B_μ (K)	k (W/m-K)
1	LiF-BeF_2	1.16E-4[a]	3755[a]	1.1[b]
2	$NaBF_4$-NaF	8.77E-5[c]	2240[c]	0.5[a]
3	LiF-NaF-KF	4.0E-5[d]	4170[d]	0.8[e]
4	NaF-ZrF_4	7.09E-5[d]	4168[d]	1[b]

a. From Cantor et al. (1968).
b. From Williams (2004).
c. From Cantor (1973).
d. From Powers (1963).
e. Average of the values reported by Williams (2004).

Cantor et al. (1968) present correlations for the surface tension, σ, that have the form

$$\sigma = A_\sigma (T - 273.15) + B_\sigma \tag{32}$$

where A_σ and B_σ are constants that vary between salts. The uncertainty is estimated to be +30,-10% for LiF-BeF_2 and ±30% for $NaBF_4$-NaF. Correlations were not available for the other molten salts. The constants for the surface tension are given in Table 8.

Table 8. Constants for surface tension.

Salt	Composition	A_σ (N/m-K)	B_σ (N/m)
1	LiF-BeF_2	-1.2E-4[a]	0.260[a]
2	$NaBF_4$-NaF	-7.5E-5[a]	0.130[a]
3	LiF-NaF-KF	NA[b]	NA[b]
4	NaF-ZrF_4	NA[b]	NA[b]

a. From Cantor et al. (1968).
b. Not available. The constants were set to the values for LiF-BeF_2.

Measurements or correlations were not found for the transport properties of salt vapors. Consequently, the transport properties are based on Chapman-Enskog theory of gases at low density (Bird et al. 1960). The dynamic viscosity of the i^{th} vapor component, μ_i (in Pa-s), is given by

$$\mu_i = 2.6693 \times 10^{-6} \frac{\sqrt{M_i T}}{\sigma_i^{\,2} \Omega_i} \quad , \tag{33}$$

where M_i is the molecular weight given in Table 2, σ_i is the collision diameter of the molecule in $\overset{o}{A}$, and Ω_i is a slowly varying function of dimensionless temperature, $T / \left(\frac{\varepsilon}{K} \right)_i$, given in Table B-2 of Bird et al. (1960), where $\left. \frac{\varepsilon}{K} \right|_i$ is the potential constant.

Values for the collision diameter and the potential constant were estimated from empirical relationships given by Bird et al. (1960). The empirical estimates were

$$\left. \frac{\varepsilon}{K} \right|_i = 1.92 T_{melt} \tag{34}$$

and

$$\sigma_i = 1.222 \, \tilde{V}^{1/3} \quad , \tag{35}$$

where $\tilde{V}$ is the volume of the solid at the melting point (in cm^3/mole). The parameters used in calculating the dynamic viscosity of each vapor component are summarized in Table 9. For convenience, Table 8 repeats the molecular weight and specific heat capacity values given in Table 2.

Table 9. Parameters used for calculating the dynamic viscosity of the vapor components.

Component	M_i (g/mole)	$\tilde{c}_{P_i}$ (J/mole-K)	T_{melt} [a] (K)	$\tilde{V}$ [b] (cm^3/mole)	$\left. \frac{\varepsilon}{K} \right|_i$ [c] (K)	σ_i [c] ($\overset{o}{A}$)
LiF	25.939	36.888	1121.3	13.61	2153	2.92
BeF_2	47.009	58.728	825	22.78	1584	3.46
$NaBF_4$	109.808	112.989	680	52.90	1306	4.59
NaF	41.988	37.699	1269	20.48	2436	3.34
KF	58.097	37.846	1131	28.90	2172	3.75
ZrF_4	167.214	105.459	1205	51.09	2314	4.53

a. From Chase (1998), except that the value for $NaBF_4$ was obtained from Cantor et al. (1968).
b. The specific volume was generally estimated from the liquid density equations given by Lide (1997), multiplied by a factor of 0.95 to account for expansion on melting. The factor of 0.95 was based on a value given by Cantor (1973) for $NaBF_4$-NaF. The specific volumes for $NaBF_4$ and ZrF_4 were extrapolated from values given by Cantor (1973). The specific volume for $NaBF_4$ was multiplied by 0.95 to account for expansion on melting.
c. From Equations (34) and (35).

The dynamic viscosity of the vapor mixture, μ_{mix} , is calculated using the formulas given by Bird et al. (1960)

$$\mu_{mix} = \sum_{i=1}^{n} \frac{X_i \mu_i}{\sum_{j=1}^{n} X_j \Phi_{ij}} \tag{36}$$

and

$$\Phi_{ij} = \frac{1}{\sqrt{8}} \left(1 + \frac{M_i}{M_j} \right)^{-1/2} \left(1 + \left(\frac{\mu_i}{\mu_j} \right)^{1/2} \left(\frac{M_j}{M_i} \right)^{1/4} \right)^2 , \tag{37}$$

where n is the number of components and μ_i and μ_j are the viscosity of components i and j respectively.

The thermal conductivity of the i^{th} vapor component, k_i in W/m-K, is given by the Eucken equation for a polyatomic gas at low density (Bird et al. 1960)

$$k_i = 1000 \left(\tilde{c}_{P_i} + \frac{5}{4} \overline{R} \right) \frac{\mu_i}{M_i} \quad , \tag{38}$$

where the molar specific heat capacity and molecular weight are given in Table 9 and the viscosity is obtained from Equation (33). The thermal conductivity of the mixture, k_{mix} , is calculated using the formula given by Bird et al. (1960)

$$k_{mix} = \sum_{i=1}^{n} \frac{X_i k_i}{\sum_{j=1}^{n} X_j \Phi_{ij}} \tag{39}$$

where Φ_{ij} is calculated from Equation (37).

The transport properties for the molten salts in ATHENA are represented in the 'new' format (Davis et al. 2004), in which the transport properties are contained in the 'tpf' files, rather than in the 'old' format, in which the transport properties are calculated in Subroutines 'viscos', 'thcond', and 'surftn'.

3. VERIFICATION

The verification of the thermodynamic properties is discussed in Section 3.1. The verification of the transport properties is discussed in Section 3.2.

3.1 Thermodynamic Properties

The thermodynamic properties for LiF-BeF_2 implemented into ATHENA were verified by comparisons with properties obtained with the generator developed by Moore (2000) that used the soft-sphere model of Chen et al. (1992a). Liquid properties obtained with Equations (1) through (14) are compared with results from the soft-sphere model in Figures 1 through 6. The specific internal energy and the specific entropy from the soft-sphere model were adjusted so that they were zero at the melting point as assumed in Equations (11) and (14). Overall, the results obtained with the simple generator were in reasonable agreement with those obtained with the soft-sphere model. The maximum deviations in the primary variables of specific volume and specific internal energy were 5% and 1%, respectively. As expected, the deviations in the derivatives of the specific volume were larger than those of the specific volume, but were still considered acceptable. The maximum deviations in the coefficient of thermal expansion and isothermal compressibility were 37% and 16%, respectively. The maximum deviation in the specific heat capacity at constant pressure was 6%. The maximum deviation in the specific entropy was 1%.

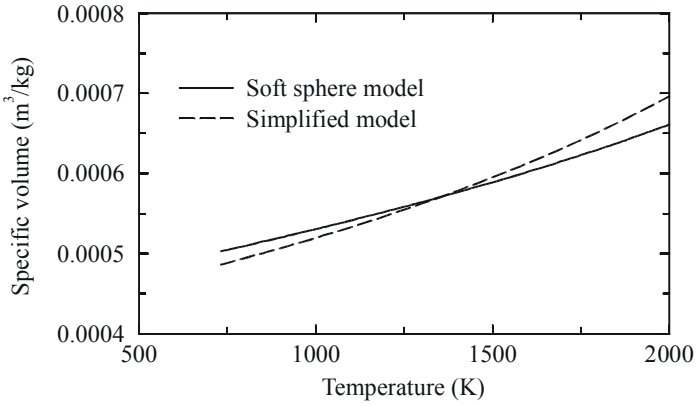

Figure 1. Specific volume of saturated LiF-BeF_2 liquid.

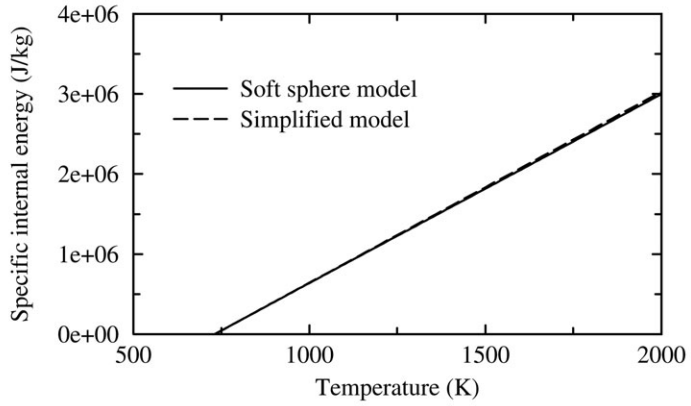

Figure 2. Specific internal energy of saturated LiF-BeF_2 liquid.

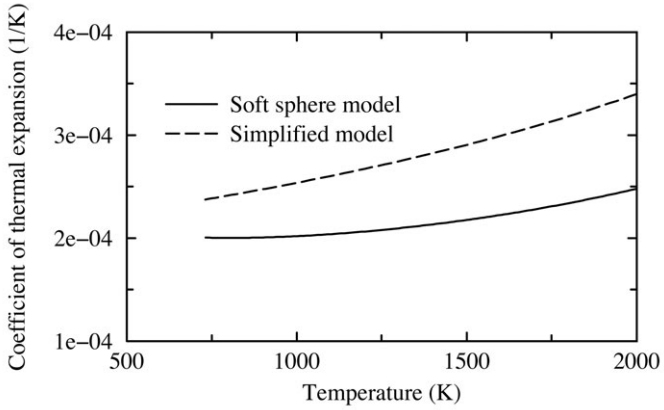

Figure 3. Coefficient of thermal expansion of saturated LiF-BeF_2 liquid.

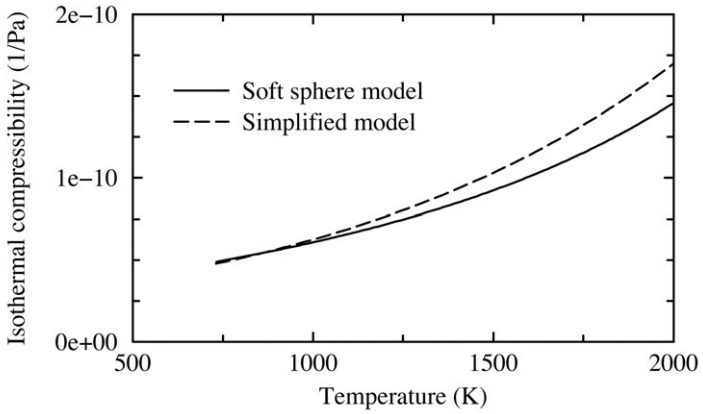

Figure 4. Isothermal compressibility of saturated LiF-BeF_2 liquid.

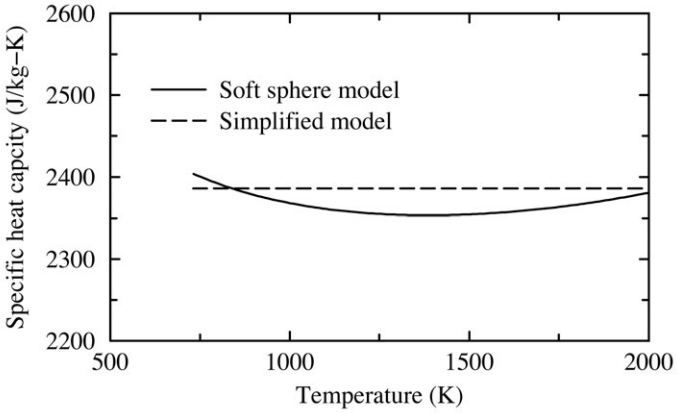

Figure 5. Specific heat capacity at constant pressure of saturated LiF-BeF_2 liquid.

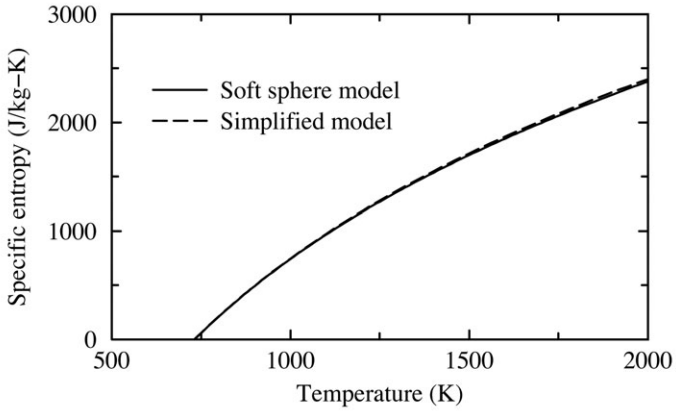

Figure 6. Specific entropy of saturated LiF-BeF_2 liquid.

The results obtained with the simple generator for LiF-BeF_2 vapor were not in as good agreement with the soft-sphere model as those presented previously for liquid. This is to be expected because of the lack of underlying measurements for vapor. Figure 7 compares the specific volume predicted by the simplified model with that obtained from the soft-sphere model. Although the trends with respect to temperature were similar with both models, the specific volume predicted by the simplified model was about three times greater than that predicted by the soft-sphere model. This discrepancy was caused by the use of different molecular weights, which resulted in different gas constants. Chen et al. (1992a) treated the salt as a compound consisting of two molecules of LiF and one molecule of BeF_2, resulting in a molecular weight of 98.89 g/mole. The approach used here was to treat the salt as a mixture of LiF and BeF_2 which yields a molecular weight of 33.1 g/mole as shown in Table 3. This approach is consistent with that used by Cantor (1973) and Powers et al. (1963) and should give a better representation of the salt vapor, which is a mixture of LiF and BeF_2. Note that Chen et al. (1992a) were interested in the properties of the liquid salt, and not the vapor. Also note that the assumption made here (that the composition of the vapor is the same as that of the liquid) is not generally correct for a binary mixture. Consequently, the uncertainties in vapor properties are expected to be relatively large. However, as mentioned previously, predictions of vapor properties are not expected to be important for NGNP applications.

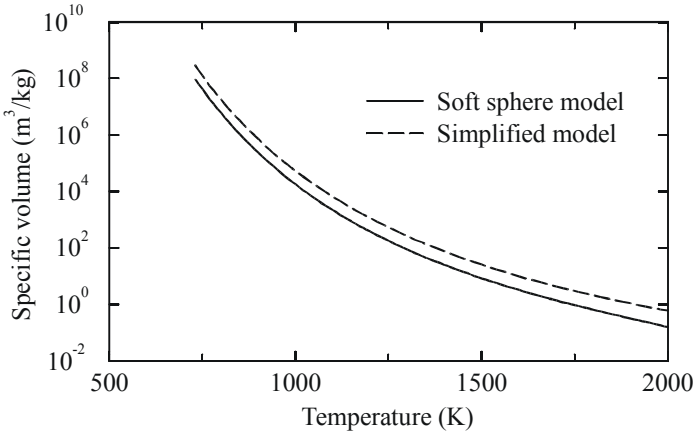

Figure 7. Specific volume of saturated LiF-BeF_2 vapor.

Figure 8 compares the specific internal energy of the vapor predicted by the simplified model with that obtained from the soft-sphere model. The primary difference between models is that

about three times more energy is required to convert the liquid into vapor in the soft-sphere model. The results from the soft-sphere model are probably more accurate because the amount of energy required to vaporize the liquid at atmospheric pressure was used in the development of the fitting coefficients for the soft-sphere model. The lower value used here was a consequence of trying to obtain the same vapor and liquid values at the estimated critical point. Although more accurate results could have been obtained for LiF-BeF_2 using values from the soft-sphere model, the approach taken here was to apply a simple approach that could be used for all four salts. As a consequence, the results from the simplified model are not expected to be accurate during boiling, but boiling should not occur during NGNP applications.

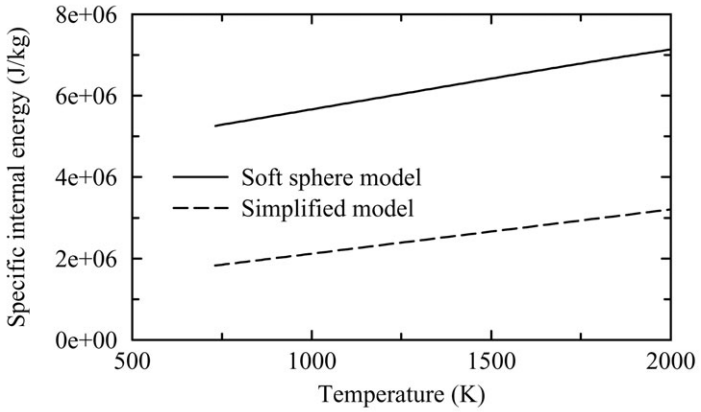

Figure 8. Specific internal energy of saturated LiF-BeF_2 vapor.

The other thermodynamic properties for the LiF-BeF_2 vapor are shown in Figures 9 through 12. The maximum deviations in the coefficient of thermal expansion and isothermal compressibility occurred near 2000 K and were 20% and 40%, respectively. The maximum deviation for the specific entropy was 70%. The different trends calculated for the specific entropy were caused by the different molecular weights discussed previously.

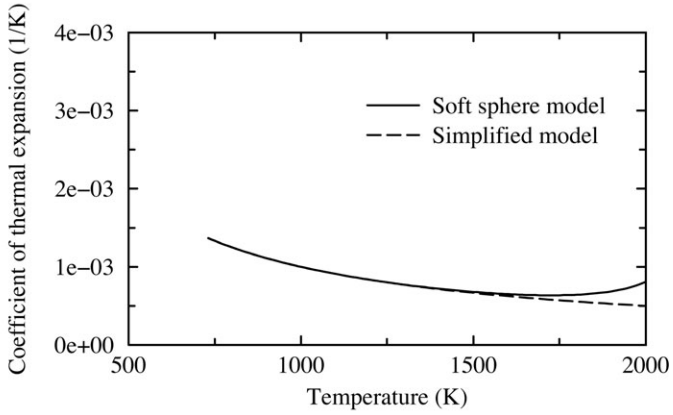

Figure 9. Coefficient of thermal expansion of saturated LiF-BeF_2 vapor.

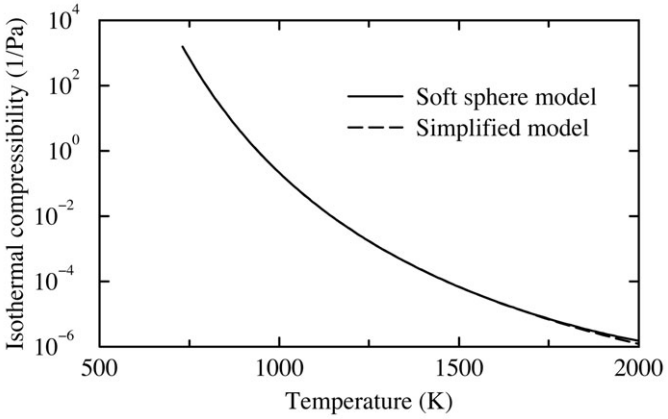

Figure 10. Isothermal compressibility of saturated LiF-BeF_2 vapor.

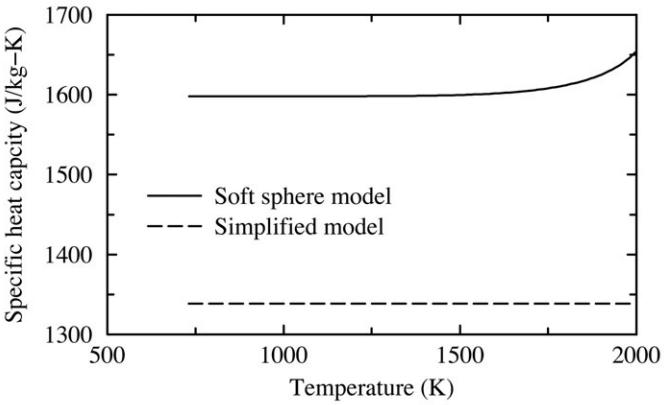

Figure 11. Specific heat capacity at constant pressure of saturated LiF-BeF_2 vapor.

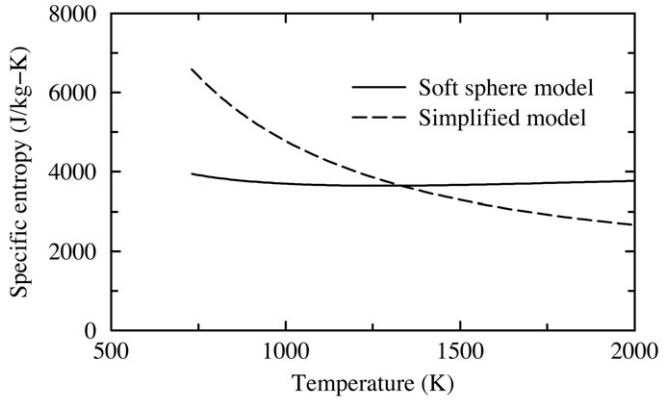

Figure 12. Specific entropy of saturated LiF-BeF_2 vapor.

The implementation of the other salts was verified by comparing the output of the simplified ATHENA generator with hand calculations using Equations (1) through (29). The comparisons showed agreement to at least five significant digits. The properties for the four liquid salts are compared in Figures 13 through 18. Figures 19 through 24 compare properties for the vapors. The saturation lines are compared in Figure 25. Properties of LiF-BeF_2 were used when correlations were not available for individual salts.

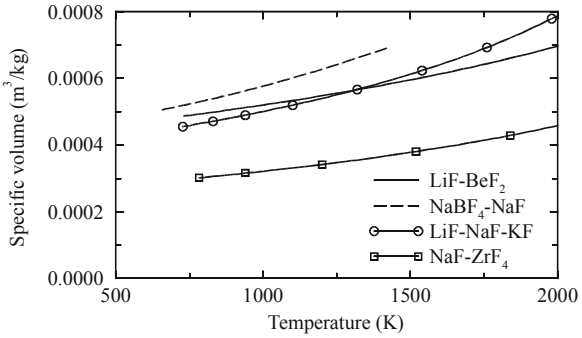

Figure 13. Specific volume of saturated liquids.

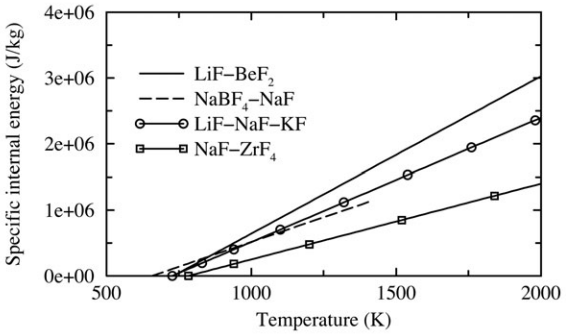

Figure 14. Specific internal energy of saturated liquids.

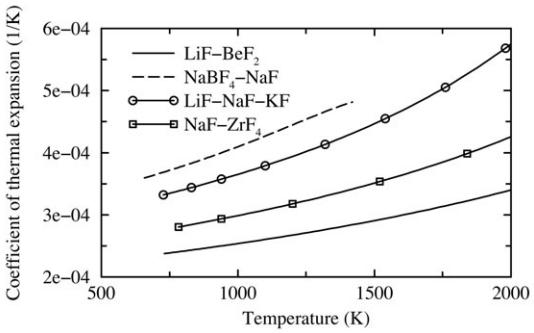

Figure 15. Coefficient of thermal expansion of saturated liquids.

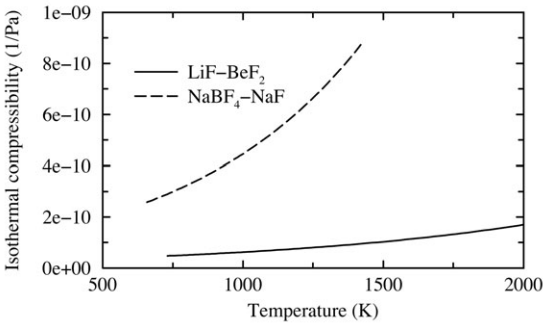

Figure 16. Isothermal compressibility of saturated liquids.

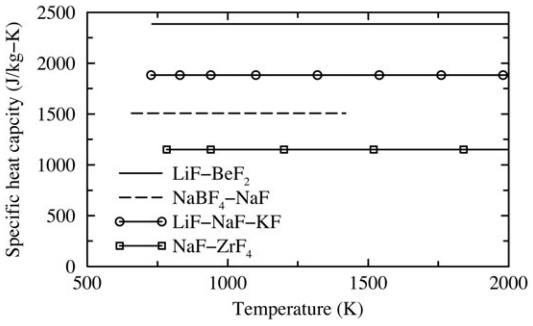

Figure 17. Specific heat capacity of saturated liquids.

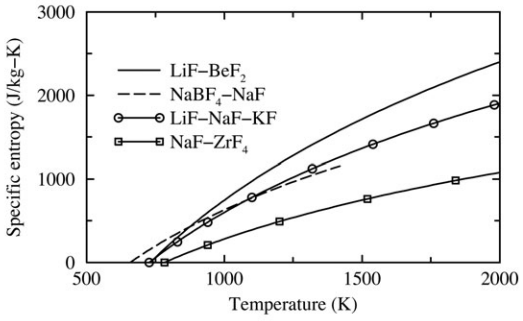

Figure 18. Specific entropy of saturated liquids.

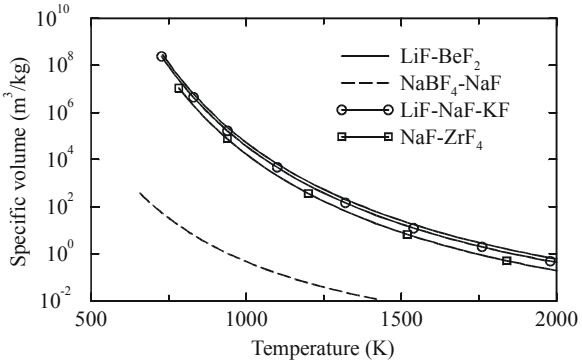

Figure 19. Specific volume of saturated vapors.

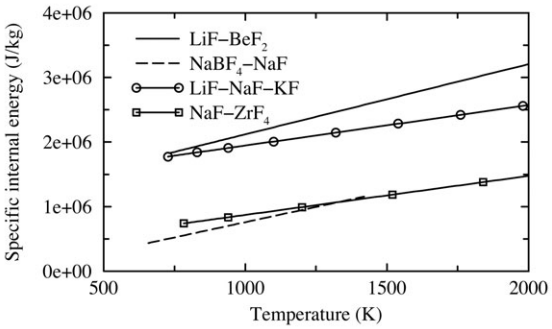

Figure 20. Specific internal energy of saturated vapors.

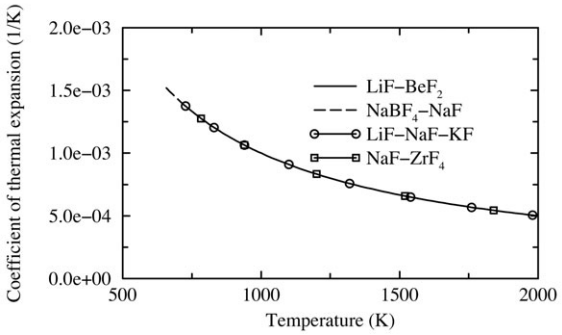

Figure 21. Coefficient of thermal expansion of saturated vapors.

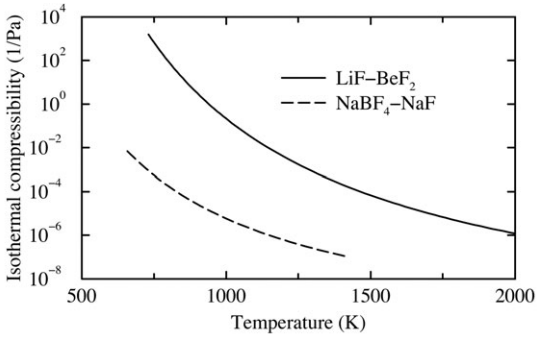

Figure 22. Isothermal compressibility of saturated vapors.

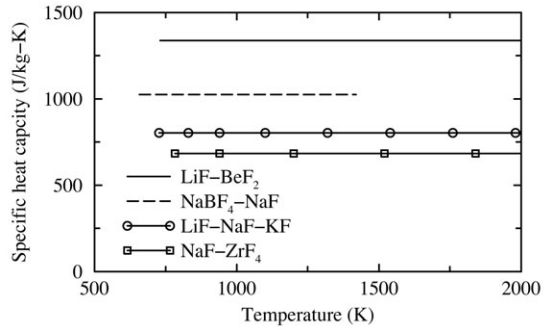

Figure 23. Specific heat capacity of saturated vapors.

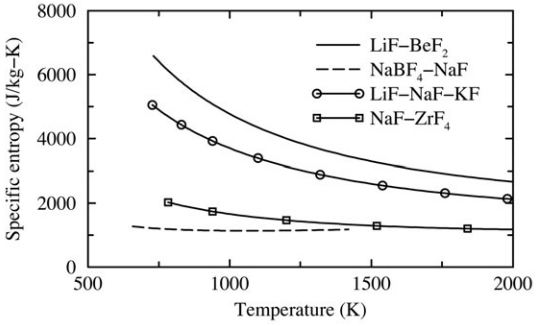

Figure 24. Specific entropy of saturated vapors.

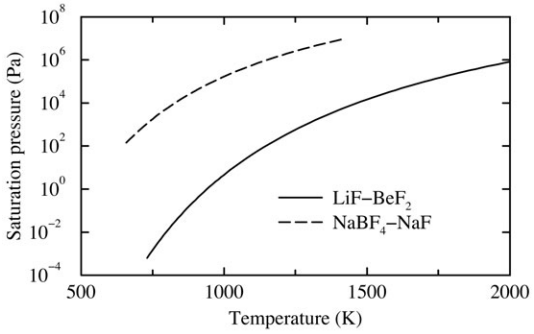

Figure 25. Saturation lines for the molten salts.

3.2 Transport Properties

The implementation of the transport properties for the salts was verified by comparing the output of the simplified ATHENA generator with hand calculations using Equations (31) through (39). The comparisons showed agreement to at least five significant digits. The transport properties of the liquids are based on measurements and expected to be within the uncertainties described in Section 2.4. However, no data are available for comparison with the calculated transport properties of the vapor. Large uncertainties are possible. Furthermore, approximate methods were used to obtain the potential constant and collision diameter used in Equation (33). Chen et al. (1992b) reported values of the potential constant and collision diameter that were about 78% and 65% of the values shown in Table 9 for LiF and BeF_2, but corresponding values could not be located for the other components. The dynamic viscosity and thermal conductivity of LiF-BeF_2 would have been almost three times larger if the values of Chen et al. had been used here. Although large uncertainties are expected in the calculated transport properties because of the lack of experimental data, the uncertainties should not be important for NGNP applications, where liquid conditions are expected.

The transport properties for the liquid salts are compared in Figures 26 and 27. Figures 28 and 29 compare vapor properties. The surface tension is shown in Figure 30. Properties of LiF-BeF_2 were used when correlations were not available for individual salts.

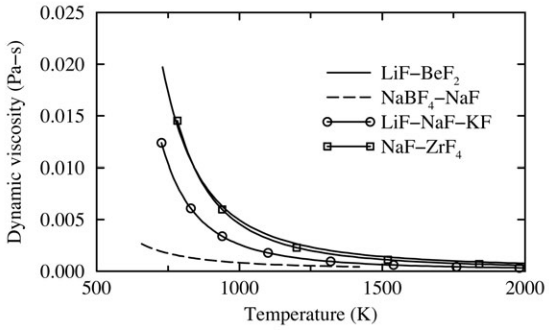

Figure 26. Dynamic viscosity of the liquid salts.

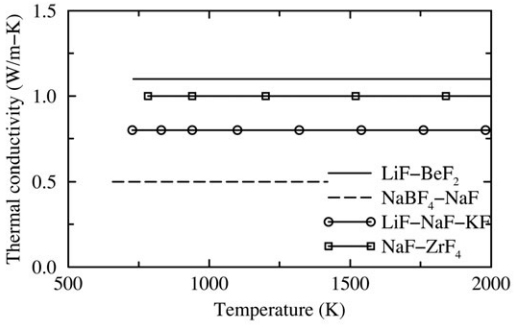

Figure 27. Thermal conductivity of the liquid salts.

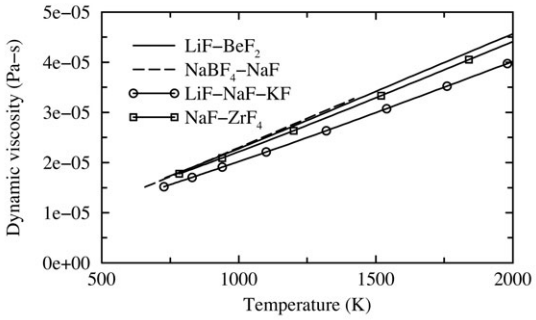

Figure 28. Dynamic viscosity of the vapors.

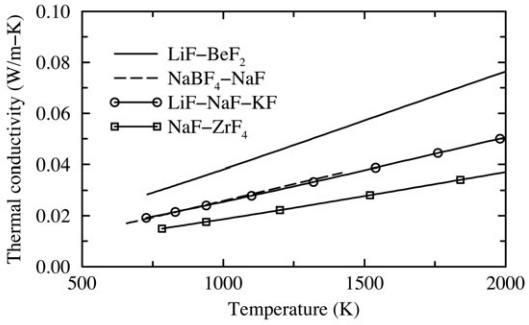

Figure 29. Thermal conductivity of the vapors.

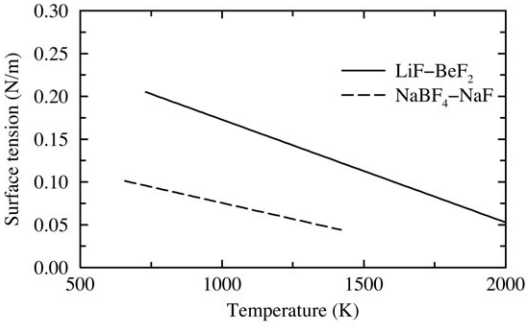

Figure 30. Surface tension.

4. CODE MODIFICATIONS

Several modifications were made to ATHENA to represent the new molten salts, which are internally referred to as 'Fluid 23', 'Fluid 24', 'Fluid 25', and 'Fluid 26'. New files were added to the fluids directory including 'stgms.F' and 'stgms1.F', which generate property tables for the first molten salt, and 'stgms1.i', which contains the input pressures and temperatures. The 'stgms.F' file is used in the property generation for all the molten salts, while the unique data required for the first molten salt is contained in the 'stgms1.F' file. The file named 'dstgxxx' in the fluids directory was modified to combine the 'stgms1.F' and 'stgms.F' files into a single file, compile and load it to create the executable file 'stgms1.x', and then execute it to generate the output files 'tpfms1' and 'stgms1.pr'. The 'dstgxxx' file was also modified to create the fluid property and output files for the other molten salts, which are named similarly to the first molten salt.

Further modifications were performed so that 'ms1', 'ms2', 'ms3', and 'ms4' are valid input selections. In the relap directory, the common deck files 'mxnfcd.H' and 'stcblkc.H' were modified as were the subroutines 'blkdta.F' and 'gninit1.F'. The subroutines that make calls to the various state routines were also modified to allow Fluids 23 through 26 to be used. These subroutines include 'dittus.F', 'mhdfwf.F', 'surftn.F', 'viscos.F', 'thcond.F', 'bishop.F', 'chfitr.F', 'chfcal.F', 'chforn.F', 'fwdrag.F', 'gcsub.F', 'gctpm.F', 'gniel.F', 'ivlvel.F', 'jacksn.F', 'ncprop.F', 'noncnd.F', 'petukv.F', 'pintfc.F', 'prebun.F', 'prednb.F', 'pstdnb.F', 'sieder.F', 'htrcn2.F', 'vexplt.F', 'vlvela.F', 'istate.F', 'stacc.F', 'stateq.F', 'jchoke.F', 'tstate.F', and 'statep.F'.

The user can select a molten salt as a working fluid in a hydrodynamic system by entering 'ms1', 'ms2', 'ms3', or 'ms4' as the third input word on the Hydrodynamic System Control Cards (Cards 120 through 129). The property files are attached as 'tpfms1' for the first molten salt (LiF-BeF_2), 'tpfms2' for the second molten salt ($NaBF_4$-NaF), 'tpfms3' for the third molten salt (LiF-NaF-KF), and 'tpfms4' for the fourth molten salt (NaF-ZrF_4).

5. QUALITY ASSURANCE

The method used to calculate the properties for the molten salts was independently reviewed. This review included checking the equations and the input and output contained in the various tables of this document. The liquid properties predicted by the generator for LiF-BeF_2 were verified as described in Section 3. The property predictions for the other salts were verified by determining that the input data contained in the 'blkdat' routine of the generator for each salt was consistent with the data contained in the tables. The vapor properties predicted by the generator were not specifically reviewed because they are relatively uncertain and not important for NGNP applications.

6. CONCLUSIONS

Four molten salts were added to the RELAP5-3D/ATHENA computer code to support analysis of the NGNP. The molten salts include LiF-BeF_2 in a molar mixture that is 66% LiF and 34% BeF_2, respectively, $NaBF_4$-NaF (92% and 8%), LiF-NaF-KF (11.5%, 46.5%, and 42%), and NaF-ZrF_4 (50% and 50%). The first and fourth salts are currently being considered for the primary coolant in the Advanced High-Temperature Reactor. The second and third salts are being considered for the heat transport loop in the NGNP.

The molten salts were implemented into ATHENA using a simplified equation of state. Liquid properties were based on correlations obtained from ORNL. The liquid density was assumed to be primarily a function of temperature. The specific heat capacity at constant pressure was

assumed to be constant. Vapor properties were based on perfect gas assumptions. The use of a simplified equation of state allows the property generator to be easily modified to represent other molten salts or as better thermophysical data become available for the selected salts. The simplified equation of state could also be modified to easily represent any fluid where the liquid phase was of primary interest.

The implementation of the thermodynamic properties into ATHENA for LiF-BeF_2 was verified by comparisons with results from a detailed equation of state developed that utilized a soft-sphere model. The comparisons between the simplified and soft-sphere models were in reasonable agreement for liquid. The maximum deviations were less than 6% for specific volume and specific heat capacity at constant pressure and less than 1% for specific internal energy and specific entropy. The deviations in the derivatives of the specific volume were larger than those of the specific volume itself, but were still considered acceptable. Similar results are expected for the other salts. The accuracy of the implemented liquid transport properties depends on the uncertainty in the underlying correlations, which were estimated to be 10 to 15% for dynamic viscosity and up to 50% for thermal conductivity.

The agreement for the vapor properties was not nearly as good as that obtained for liquid. Deviations in vapor properties were up to a factor of three. Large uncertainties are possible in the vapor properties because of a lack of experimental data. The simplified model used here is not expected to be accurate for boiling or single-phase vapor conditions. However, neither condition is expected during NGNP applications. Therefore, the simplified equation of state is considered acceptably accurate for the analysis of the NGNP.

The code's current heat transfer and friction factor correlations have been validated primarily for applications utilizing water as the working fluid. An evaluation should be performed to determine the applicability of these correlations for cases using a molten salt as the working fluid.

7. REFERENCES

Bird, R. B., W. E. Stewart, and E. N. Lightfoot, 1960, "Transport Phenomena," John Wiley & Sons, New York.

Cantor, S., 1973, "Density and Viscosity of Several Molten Fluoride Mixtures," ORNL-TM-4308, March.

Cantor, S., J. W. Cooke, A. S. Dworkin, G. D. Robbins, R. E. Thoma, and G. M. Watson, 1968, "Physical Properties of Molten-Salt Reactor Fuel, Coolant, and Flush Salts," ORNL-TM-2316, August.

Chase, M. W., 1998, "NIST-JANAF Thermochemical Tables," Fourth Edition, Journal of Physical and Chemical Reference Data, Monograph No. 9.

Chen, X. M., V. E. Schrock, and P. F. Peterson, 1992a, "The Soft-Sphere Equation of Sate for Liquid Flibe," *Fusion Technology*, Vol. 21, 1525-1530, May.

Chen, X. M., V. E. Schrock, and P. F. Peterson, 1992b, "The Calculation of the Kinetic Rate Constants for LiF and BeF_2," *Fusion Technology*, Vol. 21, 1536-1540, May.

Davis, C. B., W. L. Weaver, and R. A. Riemke, 2004, "Implementation of Helium-Xenon Properties into RELAP5-3D/ATHENA," R5-3D/04-10, December.

Glasstone, S. and A. Sesonske, 1967, "Nuclear Reactor Engineering," Van Nostrand Reinhold Company, New York.

INEEL, 2003, "RELAP5-3D Code Manual Volume 1: Code Structure, System Models and Solution Methods," INEEL-EXT-98-00834, Revision 2.2, October.

Ingersoll, D. T., C. W. Forsberg, L. J. Ott, D. F. Williams, J. P. Renier, D. F. Wilson, S. J. Ball, L. Reid, W. R. Corwin, G. D. Del Cul, P. F. Peterson, H. Zhao, P. S Pickard, E. J. Parma, and M. Vernon, 2004, "Status of Preconceptual Design of the Advanced High-Temperature Reactor (AHTR)," ORNL/TM-2004/104, May.

Knacke, O., O. Kubaschewski, and K. Hesselmann, 1991, "Thermochemical Properties of Inorganic Substances," Second Edition, Springer-Verlag, Berlin.

Lide, D. R., 1997, "CRC Handbook of Chemistry and Physics," CRC Press, Boca Raton.

Moore, R. L, 2000, "Flibe Thermal Properties for use with the Fusion Safety Multi-fluid Equation of State Package," INEEL/EXT-2000-00670, May.

Powers, W. D., S. I. Cohen, and N. D. Greene, 1963, "Physical Properties of Molten Reactor Fuels and Coolants," *Nuclear Science and Engineering*, Vol. 17, 200-211.

Sabharwall, P., L. Ott, and G. L. Yoder, 2004, "Physical Properties and Correlations for the Molten Salt FLIBE [2LiF-BeF2] and their Implementation in the RELAP5/ATHENA Thermal-Hydraulics Code," Oak Ridge National Lab, NSTD, August 26.

Williams, D. F., 2004, Oak Ridge National Laboratory, Personal communication.

Zemansky, M. W., 1968, "Heat and Thermodynamics," Fifth Edition, McGraw-Hill Book Company.

Zucrow, M. J. and J. D. Hoffman, 1976, "Gas Dynamics," Volume I, John Wiley & Sons, New York.